doi:10.1093/brain/awx179 BRAIN 2017: 140; 2355–2369 | 2355

BRAIN
A JOURNAL OF NEUROLOGY

Involvement of fast-spiking cells in ictal sequences during spontaneous seizures in rats with chronic temporal lobe epilepsy

Adam R. Neumann,[1,*] Robrecht Raedt,[2,*] Hendrik W. Steenland,[1] Mathieu Sprengers,[2] Katarzyna Bzymek,[1] Zaneta Navratilova,[1,3] Lilia Mesina,[1] Jeanne Xie,[1] Valerie Lapointe,[1] Fabian Kloosterman,[3,4,5] Kristl Vonck,[2] Paul A. J. M. Boon,[2] Ivan Soltesz,[6] Bruce L. McNaughton[1,7] and Artur Luczak[1,6]

*These authors contributed equally to this work.

See Lenck-Santini (doi:10.1093/awx205) for a scientific commentary on this article.

Epileptic seizures represent altered neuronal network dynamics, but the temporal evolution and cellular substrates of the neuronal activity patterns associated with spontaneous seizures are not fully understood. We used simultaneous recordings from multiple neurons in the hippocampus and neocortex of rats with chronic temporal lobe epilepsy to demonstrate that subsets of cells discharge in a highly stereotypical sequential pattern during ictal events, and that these stereotypical patterns were reproducible across consecutive seizures. In contrast to the canonical view that principal cell discharges dominate ictal events, the ictal sequences were predominantly composed of fast-spiking, putative inhibitory neurons, which displayed unusually strong coupling to local field potential even before seizures. The temporal evolution of activity was characterized by unique dynamics where the most correlated neuronal pairs before seizure onset displayed the largest increases in correlation strength during the seizures. These results demonstrate the selective involvement of fast spiking interneurons in structured temporal sequences during spontaneous ictal events in hippocampal and neocortical circuits in experimental models of chronic temporal lobe epilepsy.

1 Department of Neuroscience, Canadian Centre for Behavioural Neuroscience, University of Lethbridge, 4401 University Dr W, Lethbridge, AB, T1K 3M4, Canada
2 Department of Neurology, Ghent University, Gent, Belgium
3 Neuro-Electronics Research Flanders, Leuven, Belgium
4 VIB, Leuven, Belgium
5 Brain and Cognition Research unit, KU Leuven, Leuven, Belgium
6 Department of Neurosurgery, and Stanford Neurosciences Institute, Stanford University, Stanford, CA, USA
7 Department of Neurobiology and Behavior, University of California at Irvine, Center for the Neurobiology of Learning and Memory, Irvine, CA, USA

Correspondence to: Artur Luczak
Department of Neuroscience, Canadian Centre for Behavioural Neuroscience, the University of Lethbridge, 4401 University Dr W, Lethbridge, AB, T1K 3M4, Canada
E-mail: Luczak@uleth.ca

Correspondence may also be addressed to: Bruce L. McNaughton
E-mail: Bruce.McNaughton@uleth.ca

Keywords: temporal lobe epilepsy; neuronal population activity, GABAergic cells

Received February 16, 2017. Revised May 25, 2017. Accepted June 8, 2017. Advance Access publication August 4, 2017.

Abbreviations: KA = kainic acid injection model; LFP = local field potential; PP = perforant path stimulation model; TLE = temporal lobe epilepsy

Introduction

Epilepsy is one of the most prevalent neurological disorders affecting over 1% of the general population (Thurman *et al.*, 2011). Among adult patients, temporal lobe epilepsy (TLE) is the most common subtype of epilepsy (Wiebe, 2000). The treatment of TLE is often difficult, most likely due to complexity of molecular, cellular and synaptic mechanisms causing microcircuit alterations at multiple levels. To better understand the mechanisms responsible for TLE, several animal models of this disorder have been developed (Kandratavicius *et al.*, 2014; Lévesque *et al.*, 2016*a*), which have provided a number of important insights into TLE. Aided by technological advancements allowing continuous monitoring of the activity of large sets of individual neurons in humans as well as in animals, our understanding of complex neuronal dynamics involved in epileptic networks has significantly improved. For example, application of multi-electrode single-unit recordings revealed that ictal events have a rather heterogeneous pattern of activity (Truccolo *et al.*, 2011, 2014; Bower *et al.*, 2012; Cymerblit-Sabba and Schiller, 2012), instead of the seemingly homogeneous recurrent discharges suggested by the synchronous EEG patterns during seizures. Further evidence of heterogeneous ictal dynamics was also indicated by two-photon calcium imaging in hippocampal slices from chronically epileptic animals exhibiting spontaneous seizures (Muldoon *et al.*, 2013), revealing that epileptic networks may be composed of multiple functional clusters of spatially localized neurons. Interestingly, despite this heterogeneity of spiking patterns within seizures, neuronal activity patterns were also found to be remarkably similar across consecutive seizures (Truccolo *et al.*, 2011). Taken together, these results suggest that although neuronal dynamics during seizures is likely to be complex, it may have consistent underlying mechanism.

Dynamics of neuronal patterns cannot be fully understood without considering the role of inhibition. Indeed, GABAergic cells are not only implicated in keeping cellular and network excitation in check, but are also critically involved in generating and coordinating behaviourally relevant neuronal oscillations (e.g. hippocampal theta, gamma, and ripple oscillations) across various temporal and spatial scales (Cardin *et al.*, 2009; Varga *et al.*, 2012; Stark *et al.*, 2014). Given their functional importance in the normal brain, it is not surprising that GABAergic neurons also play key, albeit multifaceted, complex roles in epileptic networks. For example, GABAergic processes are likely to at least partially keep the balance of excitation and inhibition in check even in the epileptic brain (Prince, 1968; Velazquez and Carlen, 1999; Cohen *et al.*, 2002). Moreover, inhibition adjacent to an active focus was reported to exert a restraining role against the spread of epileptiform discharges (Prince and Wilder, 1967) in both human epilepsy and in seizure models (Trevelyan *et al.*, 2006; Sabolek *et al.*, 2012; Schevon *et al.*, 2012; Trevelyan and Schevon, 2013). On the other hand, multiple lines of evidence suggest more complex roles for GABAergic processes beyond the dampening of epileptic activity. For example, while some parameters of GABAergic transmission appear to indicate a weakened state of inhibition, numerous other reports show a paradoxical strengthening of GABAergic synaptic and cellular actions in case of epilepsy (Chen *et al.*, 2001; Cossart *et al.*, 2001; Marchionni and Maccaferri, 2009). A particularly striking example of the latter scenario has come from a recent *in vivo* cellular resolution imaging study that found GABAergic neurons, and not their glutamatergic counterparts, to be preferentially recruited during spontaneous interictal activity in the CA1 region of the epileptic mouse hippocampus in chronic experimental TLE (Muldoon *et al.*, 2015). Specifically, the latter *in vivo* two-photon calcium imaging study showed that spontaneous interictal spikes in the CA1 network recruited subsets of GABAergic neurons, which, in turn, appeared to synchronously inhibit the excitatory pyramidal cells, reducing their firing rate. However, it has not been studied in depth if the counterintuitively enhanced inhibitory activity reported to take place during interictal spikes in an experimental model of TLE may also be present during ictal spikes.

We used population recordings in two rat models for chronic TLE to show that ictal spikes were accompanied by characteristic, sequential patterns of neuronal activity, which were highly conserved across seizures. Similar sequential relations between subsets of neurons were also present before seizures. Moreover, during ictal spikes, characteristic neuronal dynamics was observed, with close temporal coupling preferentially emerging among a subset of neurons that already had the strongest correlated activity even before seizure. Importantly, neurons that were strongly activated during ictal events were predominantly the fast-spiking units, representing putative interneurons, and not excitatory principal cells as previously thought. Taken together, the results reported in this study reveal repeating patterns of neuronal activity during ictal events and, building on recent discoveries concerning the strong involvement of interneurons in interictal spikes (Muldoon *et al.*, 2015), also demonstrate the strong involvement of hippocampal and neocortical non-principal cells during chronic seizure events in experimental models of TLE.

Materials and methods

All experiments were carried out in accordance with protocols approved by the Animal Welfare Committees of the University of Lethbridge and Ghent University.

Hyperdrive implantation

In our experiments, two different rat models of chronic TLE were used: the perforant path stimulation (PP) model, and the intrahippocampal kainic acid (KA) model (see below for details). Starting 4 weeks after electrical (PP) or chemical (KA) status epilepticus induction, all animals were monitored for the presence of spontaneous seizures during 5 days of continuous video-EEG monitoring sessions. Four male Sprague-Dawley rats (three PP and one KA), which had the highest number of behavioural seizures (stage 3 or higher on the Racine Scale) (Racine, 1972; Raedt *et al.*, 2009) were selected for implantation of a multi-tetrode hyperdrive. Hyperdrives were similar in design to those previously described (Gothard *et al.*, 1996; McNaughton, 1999). Tetrodes were made by twisting four 13 µm wires together (Gray *et al.*, 1995). Tetrodes with short-circuited individual wires were used as a reference.

The rats were anaesthetized with isoflurane (1–1.5% and 1–2 l/min oxygen) and the dental cement was removed from the region over the right hemisphere where the hyperdrive was to be positioned. The exact location of the hyperdrive (3.8 mm posterior and 2 mm right to bregma) was marked on the skull using a drill bit during the first implantation surgery since bregma was no longer visible due to the presence of a dental acrylic head cap. A craniotomy was made at the marker location, the dura mater was carefully removed and the hyperdrive was positioned on the surface of the cortex. Immediately after affixing the hyperdrive to the skull and the existing head-cap using dental cement, all tetrodes were slowly lowered 1 mm below cortical surface. A 14-tetrode hyperdrive was implanted in one epileptic PP rat, and a 21-tetrode hyperdrive was implanted in two PP rats and one KA rat.

Epilepsy induction and monitoring

Perforant path stimulation model

Rats were anaesthetized with isoflurane (1–1.5% and 1–2 l/min oxygen), and bipolar stimulation electrodes were implanted bilaterally in perforant path (8.1 mm posterior and 4.4 mm lateral from bregma), and a bipolar local field potential (LFP) recording electrode was implanted with 0.9 mm tip separation in dentate gyrus (3.8 mm posterior, 2 mm left of bregma). Recording and stimulation electrodes were made by twisting two Teflon®-coated annealed stainless steel wires (Medwire 316SS3T). Depth of recording and stimulation electrodes was optimized using electrophysiological control aiming at maximal dentate gyrus evoked potentials in response to perforant path stimulation (McNaughton *et al.*, 1978). Two screw electrodes were used as ground and reference electrodes, respectively. The reference and ground electrodes were placed epidurally over the frontal cortex. Seven additional anchor screws were placed (two in the frontal bone, two in the temporal bone and three in the occipital bone) to ensure fixation of the electrode assembly to the skull using dental cement. At least 1 week after surgery, the animals were stimulated for 3 h while awake, using a protocol consisting of 15–20 V paired-pulse stimuli delivered at 2 Hz, with a 40-ms interpulse interval, plus 10-s long, 20 Hz stimulus trains of single, 15–20 V stimuli delivered once per minute for 3 h (Bumanglag and Sloviter, 2008). Convulsive status epilepticus was terminated by interaperitoneal injection of a combination of diazepam (20 mg/kg) and ketamine (50 mg/kg) (Vermoesen *et al.*, 2010).

Intrahippocampal kainic acid model

To determine the generalizability and model invariance of the key findings obtained from the PP model, chronic seizures were also recorded from one rat in the KA model. The KA rat was anaesthetized with isoflurane (1–1.5% and 1–2 l/min oxygen) and bilaterally implanted with a bipolar recording electrode in the hippocampus (5.5 mm posterior and 4 mm lateral from bregma; 3.8 mm ventral from dura). An injection guide cannula was placed above the left hippocampus (5.5 mm posterior and 4 mm left from bregma; 0.5 mm ventral from dura). Two screw electrodes were used as ground and reference electrodes. The reference and ground electrodes were placed epidurally over the frontal cortex. Seven additional anchor screws were placed (two in the frontal bone, two in the temporal bone and three in the occipital bone) to ensure fixation of the electrode assembly and cannula to the skull using dental cement. At least 1 week after implantation surgery the awake rat was injected with kainic acid (0.4 µg in 0.2 µl saline, 0.1 µl/min saline, Sigma Aldrich) in the left hippocampus using a 1 µl Hamilton syringe. A 30-G needle, attached to the Hamilton syringe, was lowered through the cannula until the needle tip was positioned 5 mm below the cannula tip (5.5 mm ventral from dura). Hyperdrive tetrodes were inserted contralateral to the KA injection site.

For both models the status epilepticus was convulsive.

Histology

All rats were kept on a 12-h light/dark schedule and provided food and water *ad libitum*. To maximize stability of the recordings, tetrodes were left in place unless they lost units during the recording. Tetrode location was verified using histology (Supplementary Fig. 1). Because some of the tetrodes were moved during the recording period, their position during a specific recording epoch sometimes had to be estimated based on histology and the amount of movement performed since the recording epoch.

When recording was finished, tetrode locations were marked by making small lesions at the electrode tips with 10 µA of anodal current for 10 s. Rats were injected with Euthansol (sodium pentobarbital, intraperitoneally) and were transcardially perfused with phosphate-buffered solution (PBS) and paraformaldehyde (PFA). The brains were removed and kept in PFA for 1–2 days and then placed in 30% sucrose with sodium azide. After a few weeks, the brains were sectioned into 40-µm thick sections during block-face imaging on a custom vibratome to determine the relevant part of the brain. All sections relevant to electrode placement were triple immunostained with neuronal nuclear antigen (NeuN), vimentin, and anti-CD11b/c antibody (Ox-42) (Supplementary Fig. 1).

Electrophysiological recordings

Electrical signals from tetrodes were continuously recorded with a 128-channel Neuralynx Cheetah Acquisition System. For unit recordings, signals were digitized at 32 kHz and bandpass filtered between 600 Hz and 6 kHz. For LFP recordings, signals were digitized at 2 kHz and bandpass filtered between 1 and 1000 Hz. The reference tetrode was positioned in superficial cortical areas. The remaining tetrodes were each turned in the morning, ~50 µm per day, keeping them as close to the same depth as possible. When tetrodes reached cortical layers 5/6, about half of them were kept in place for recording of neuronal activity in parietal cortex, and the remaining tetrodes were advanced to the CA1 pyramidal cell layer—as noted by multiple, single units and polarity reversals of sharp waves (Buzsáki *et al.*, 1990). Individual recording sessions lasted ~24 h. Animals were recorded 24/7, with a short break every morning when tetrodes were adjusted and a new recording session was started.

Seizure detection

Seizures were identified on the LFP signal recorded from tetrodes located in the hippocampus. A seizure was defined as a paroxysmal occurrence of high frequency and/or high amplitude rhythmic discharges with a clear evolution of signal complexity and lasting at least 10 s. Seizure onset was manually identified as the earliest appearance of a persistent change in the signal that developed into clear seizure activity (Supplementary Fig. 2) (Bragin *et al.*, 1999). Frequently seizure onset was accompanied by a characteristic LFP deflection, such as an initial slow wave (Supplementary Fig. 2B). Note that, for analyses of seizure long patterns (Fig. 1A–D), finding the exact time of seizure onset with sub-second precision was not crucial, as neuronal activity was smoothed with a Gaussian kernel with standard deviations (SD) = 10 s. Across eight analysed datasets, the mean number of seizures within the 24-h period was 25.75 (min = 4, max = 56; KA rat had 10 and 56 seizures in the 2 days analysed, respectively) with average seizure duration of 77.25 s (min = 23, max = 182 s). The median inter-seizure interval was 82.7 min (min = 2.8, max = 537 min). If the inter-seizure interval was <10 min, then those seizures were excluded from analyses.

To detect peaks of ictal spikes, hippocampal LFP from the tetrode with the highest amplitude of ictal spikes was chosen and bandpass filtered between 5 and 150 Hz. Peaks were detected with the findpeaks MATLAB function. If more than one peak was detected within a 30-ms window, then only the peak with the highest amplitude was kept. Peaks with amplitudes <1 mV were removed. Changing this threshold to 0.5 or 1.5 mV gave qualitatively similar results.

Spike sorting

Units were isolated by a semiautomatic algorithm (KlustaKwik -1.6, available at http://klustakwik.sourceforge.net) (Harris *et al.*, 2000) followed by manual clustering (MClust 3.1; Redish, 2002; Schjetnan and Luczak, 2011). Unit quality was evaluated using an isolation distance measure (Harris *et al.*, 2000). For our analyses, we included putative single unit clusters (isolation distance >20), as well as potential multiunit clusters (~2–5 neurons) with low separation quality (isolation distance >5). We used the latter approach because putative multiunit clusters still showed cluster-specific activity patterns before and during seizures, therefore improving detection of population patterns. Restricting analyses to only well isolated units (isolation distance >20), gave qualitatively similar results. On average, we had 94.4 units (min = 21, max = 177) across eight analysed datasets (two for each rat). Because spike sorting of 24-h datasets can take weeks to finish, only datasets with the largest number of seizures and with the best recording quality were analysed. Although hyperdrives can provide stable unit recordings for periods longer than 24 h (Schwindel *et al.*, 2014), we restricted our analyses to quantify similarity of spiking patterns only between consecutive pairs of seizures to minimize effect of long-term 'drift' of units (see 'Results' section).

Although spike sorting during seizures can be especially challenging and even problematic, there are multiple studies showing that it can be done successfully (Truccolo *et al.*, 2011; Merricks *et al.*, 2015). In addition, in the current study, we provide additional evidence supporting the validity of our spike sorting techniques. First, examination of spike waveforms before, during and after seizures showed consistent spike shapes (Supplementary Figs 3 and 4). Similarly, spike features in principal component space were consistent before and during seizure (Supplementary Fig. 3B). However, the strongest evidence for identifying the same units before and during seizure is provided by our cross-correlogram analysis (see 'Results' section), showing consistent functional relations between pairs of neurons before and during seizures, which would be unlikely to obtain without having the same units in both time periods (see difference between original and neuron shuffled data in Fig. 5C).

Neuronal entrainment to local field potential and cross-correlogram calculations

To quantify neuronal entrainment to LFP, for each neuron we calculated its cross-correlogram with hippocampal LFP using the MATLAB xcorr(..'coef') function. This normalizes the autocorrelations at zero lag to 1, which enables convenient expression of values of correlogram as correlation coefficients. To account for the fact that neurons can have different time lag to LFP modulation, we used the highest value of cross-correlogram peak within −50 +50 ms as an entrainment value (Fig. 3B, inset). For those analyses, the LFP from the tetrode with the highest amplitude of ictal spikes was chosen, but selecting different hippocampal channels gave qualitatively similar results.

For cross-correlogram analyses between pairs of neurons, to account for differences in firing rates, all cross-correlograms were normalized using the formula: xcorr × L / (N1 × N2); where xcorr is cross-correlogram, L is the number of time bins within the analysed period, and N1 and N2 stand for the sum of spikes of neuron 1 and 2, respectively. After this normalization, the cross-correlation value expected by chance is 1. To make our cross-correlation plots more intuitively understandable, we subtracted 1 from all normalized cross-correlograms, thus the level of cross-correlation expected by chance was set to 0. For cross-correlogram analyses between

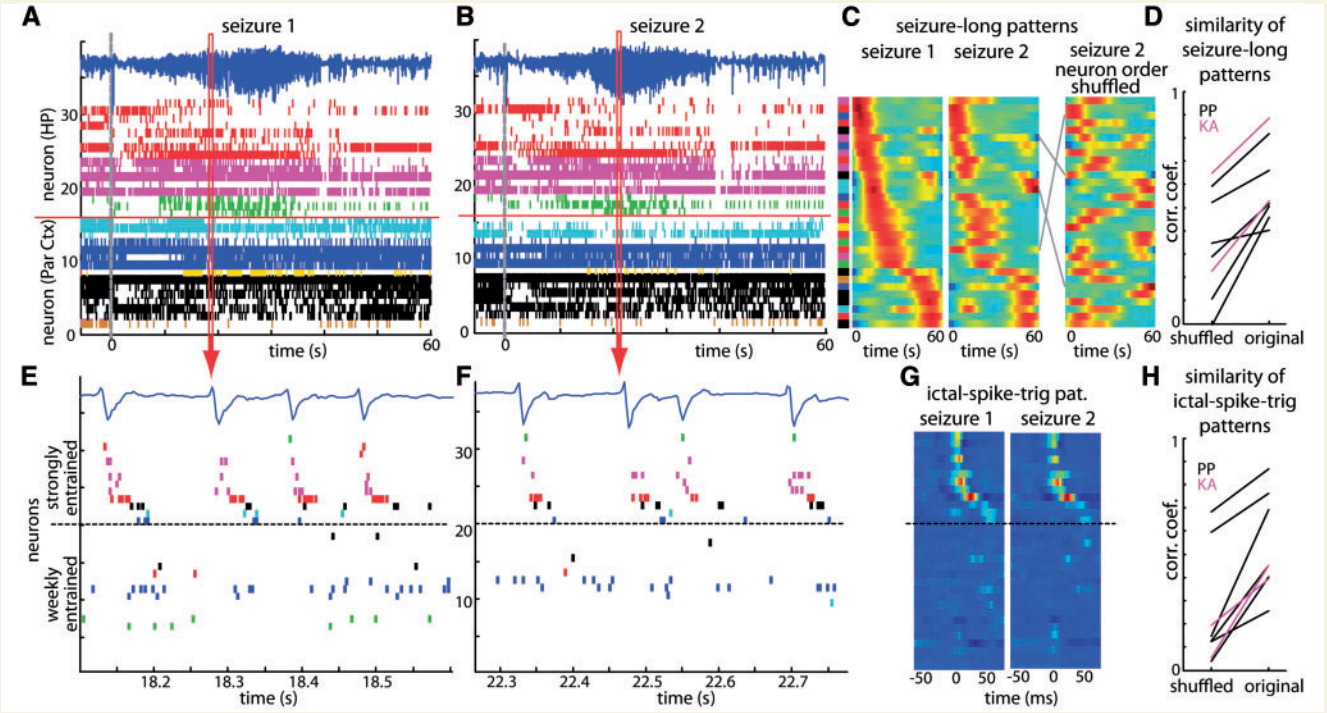

Figure 1 Consistency of neuronal firing patterns on multiple time scales across seizures. (**A** and **B**) Example of neuronal activity in hippocampus (HP) and parietal cortex (Par Ctx) for two consecutive seizures in the PP model. Neurons marked with the same colour were recorded on the same tetrode. On the *top* is the LFP from the hippocampal electrode. The grey vertical line indicates seizure start. (**C**) The same neuronal activity as in **A** and **B** but smoothed with a 10-s Gaussian kernel, z-score normalized and sorted by latency during seizure #1. Colour bar on the left shows which tetrode the neuron was recorded according to colour scheme in **A** and **B**. *Right* panel shows the same activity as the *middle* panel but with neuron order shuffled. Grey lines show position of sample neurons before and after shuffling. (**D**) Similarity of seizure-long patterns across seizures for original and neuron order shuffled data. Each line represents data from a single 24 h recording period (2 days were analysed for each of the four rats). Data for the rat in the KA model of epilepsy are marked in violet (Fig. 2). (**E** and **F**) Sample 500 ms windows of activity from seizures 1 and 2. In both plots, strongly entrained neurons are sorted by average latency to ictal spikes during seizure 1. Colour coding corresponds to colours in **A** and **B**. (**G**) Average ictal spike triggered neuronal activity for seizure 1 and 2. Neurons are sorted in the same order as in **E**. (**H**) Similarity of ictal spike triggered patterns across seizures. Plot convention was the same as in **D**. In **D** and **H**, higher values of correlation for all original datasets, as compared to shuffled data, show that seizure-long patterns as well as ictal-spike-triggered activity patterns are consistent across seizures.

single neuron and multi-unit activity the same normalization formula was used.

For all presented results, we report mean ± standard error of the mean (SEM), unless otherwise stated.

Discrimination of putative interneurons and putative pyramidal cells

Narrow-spike cells (putative fast spiking interneurons) and wide-spike cells (putative pyramidal cells) can be characterized by distinct extracellular spike waveform features. Although spike width cannot always unequivocally discriminate between interneurons and pyramidal cells, it is generally accepted that for the vast majority of neurons it is a valid and useful indicator of cell type (Fox and Ranck, 1975; Mizumori *et al.*, 1989*a*; Markus *et al.*, 1994). We used spike duration (measured as trough-to-peak time in the spike waveform) and spike half amplitude duration to determine the type of neuron as described previously (Barthó *et al.*, 2004; Luczak and Barthó, 2012). The distribution of trough-to-peak durations was approximately bimodal with a narrow border between clusters ~0.23 ms (Fig. 3A and Supplementary Fig. 5). The discrimination based on spike width at half of its maximum amplitude was less clear, although neurons with shortest half-width also had shortest trough-to-peak durations.

For verification of the spike shape based classification, we computed cross-correlograms (1 ms bin width) between all pairs of recorded neurons to identify putative inhibitory connections. Significant troughs within 3 ms of the centre bin were considered as putative monosynaptic inhibition. A trough in the cross-correlogram was defined as significant when at least two neighbouring 1 ms bins were below 3 SD of the bin values in the control period calculated between −30 to −10 ms and between +10 to +30 ms (Fig. 3A inset).

In addition, to further verify spike width-based classification, we also investigated auto-correlograms of putative interneurons and putative pyramidal cells. Pyramidal cells typically have a peak in the autocorrelogram either at ~3–5 ms reflecting bursting activity, or at much later time (>50 ms); in contrast, fast spiking interneurons tend to have peak in the

autocorrelogram between about 7–40 ms (Fig. 3A inset) (Mizumori *et al.*, 1989*b*; Barthó *et al.*, 2004). Of 755 cells in our dataset, 129 cells had auto-correlogram peak between 7 and 40 ms. Finally we also used firing rate >15 Hz as an additional feature to identify fast spiking putative interneurons (66 of 755 cells passed the latter firing rate criterion).

Results

To investigate neuronal firing dynamics in relation to spontaneous chronic seizures in the chronic phase of epilepsy, neuronal population activity in hippocampus and parietal cortex was continuously recorded in two distinct rat models of temporal lobe epilepsy (PP model: three rats; KA model: one rat).

Reproducible patterns of neuronal activity during seizures

First, we examined the overall neuronal activity patterns during seizures. Spontaneous seizures were associated with neuronal activity patterns, where some neurons were consistently active at the start of the seizures, whereas other neurons showed increased levels of discharges particularly during the later phases of the seizure (Fig. 1A). Such tens of seconds long neuronal activity patterns were highly reproducible across seizures (PP model, Fig. 1A and B; KA model, Fig. 2). To quantify the similarity of spiking patterns across seizures, we smoothed and normalized the activity of each neuron, and calculated the correlation coefficient between neuronal patterns of consecutive seizures (Fig. 1C and Supplementary Fig. 6A). Correlations expected by chance were estimated by repeating the same analysis after shuffling the order of neurons for each seizure independently (Fig. 1C) (note that shuffling the order of neurons is a more stringent test than spike-time shuffling; for example, if the majority of neurons are active at seizure start, the neuron order shuffled patterns will also have most neurons active at seizure start resulting in an above zero correlation to the original pattern; therefore, shuffling the order of neurons makes it more difficult to reject the null hypothesis as compared to spike-time shuffling; see Supplementary Fig. 7). The analysis showed that the correlations between the original activity patterns were significantly higher than correlations between neuron order shuffled patterns for all analysed datasets ($r_{orig} = 0.56 \pm 0.085$, $r_{shufl} = 0.33 \pm 0.081$, $P = 0.0011$; paired *t*-test; Fig. 1D). Thus, consistent with results found in epileptic patients (Truccolo *et al.*, 2011), we observed seizure-long, reproducible patterns of neuronal activity conserved across seizures.

Consistent sequential activity patterns during ictal spikes

Subsequently, we examined spiking patterns during seizures at much shorter time scales (~50–100 ms). We found that subsets of neurons were strongly entrained to ictal spikes, forming sequential activity patterns even across brain areas

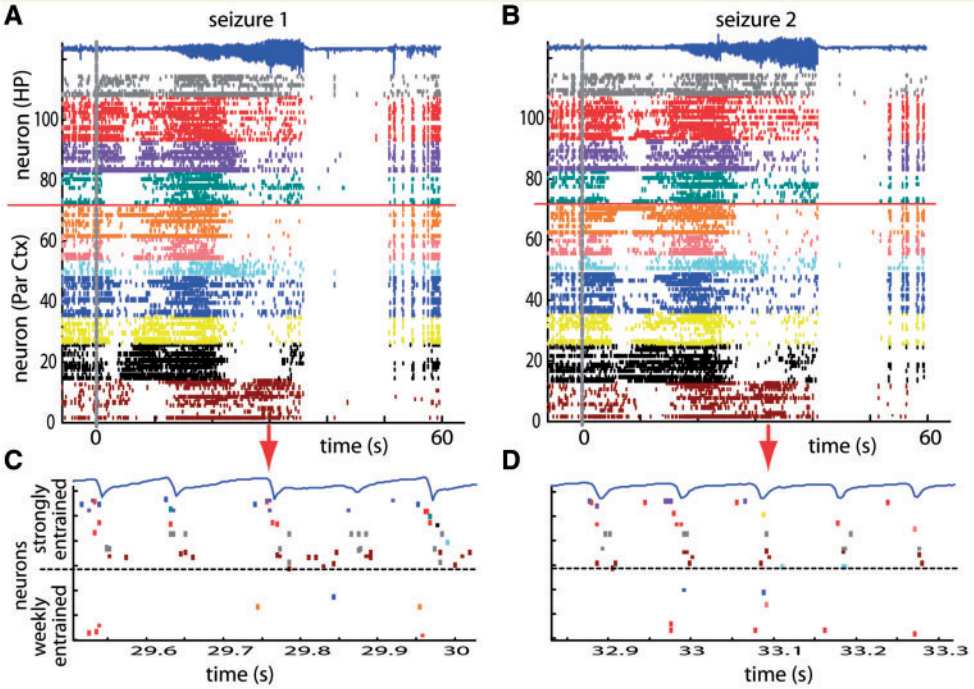

Figure 2 Model invariance. Reproducibility of long and short spiking patterns during seizures in the KA model. (**A** and **B**) Examples of long neuronal activity patterns for two consecutive seizures. (**C** and **D**) Sample 500 ms windows of activity form seizures in **A** and **B**. Plots convention is the same as in Fig. 1A, B, E and F. Note that both PP and KA models show clear long and short spiking patterns which are conserved across seizures.

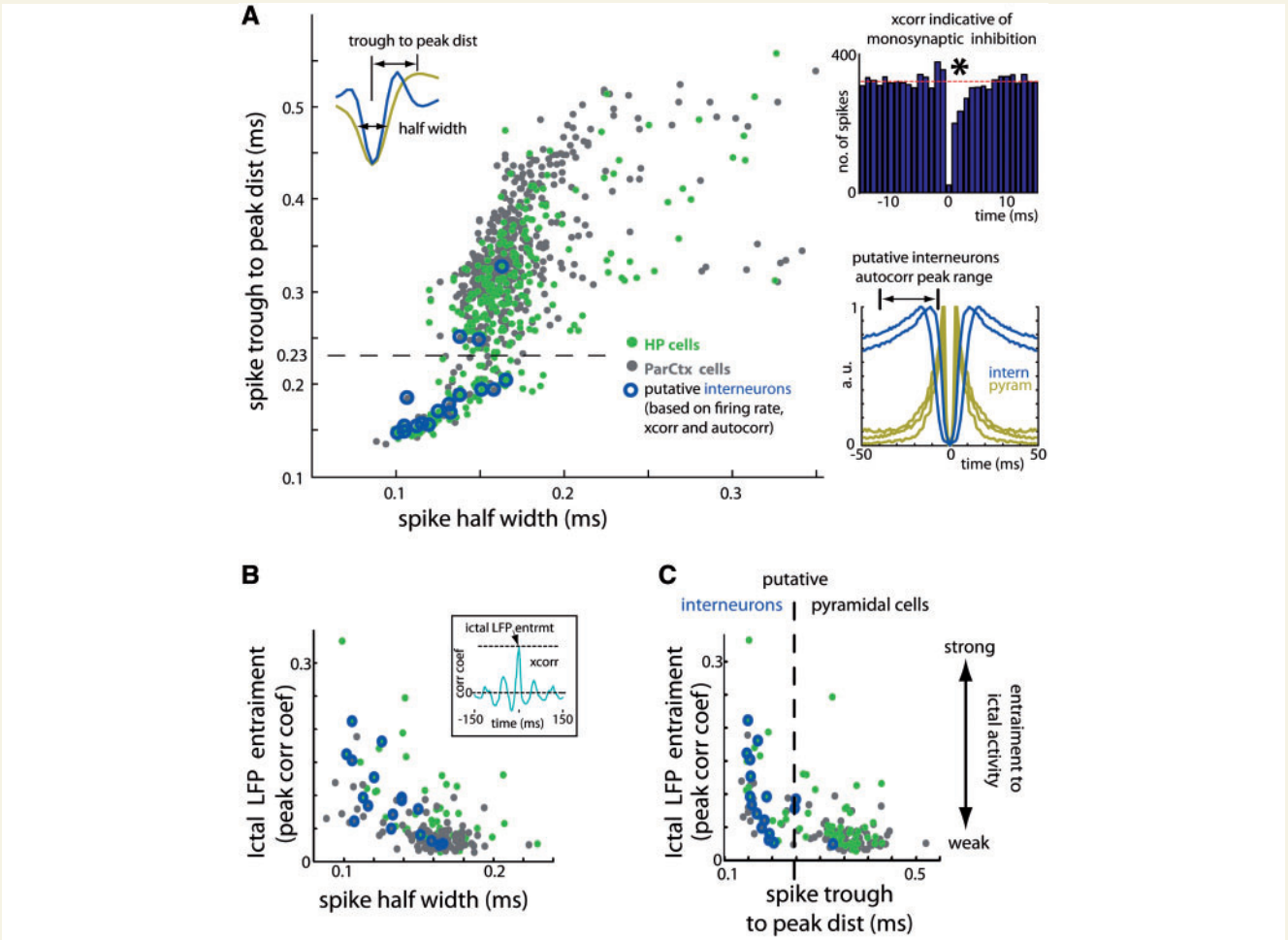

Figure 3 Ictal spikes engage predominantly putative interneurons. (**A**) Discrimination of putative interneurons from putative pyramidal cells based on spike shape (half spike width and trough-to-peak distance). Hippocampal and parietal cortex cells are marked in green and grey, respectively. Blue circles denote cells that had in conjuncture three other typical features of interneurons (firing rate >15 Hz, short latency inhibition to other cell, and most often inter-spike interval between 7 and 40 ms). *Top left inset*: Illustration or representative spike waveforms from a putative interneuron (blue) and a pyramidal cell (olive). *Top right inset*: Sample cross-correlogram between a putative interneuron and a pyramidal cell indicating short latency (monosynaptic) inhibition. Star denotes significantly lower coincidence of spikes as compared to baseline. *Bottom right inset*: Representative auto-correlograms of putative interneurons (blue) and pyramidal cells (olive). Peaks around zero are due to bursting activity characteristic of pyramidal neurons. (**B**) Relation between cell spike width and entrainment to ictal spikes (defined as height of cross-correlogram with hippocampal LFP; *inset*). Note that negative correlation between spike width and LFP entrainment shows that narrow spike cells are more strongly modulated by ictal spikes than wide spike cells. (**C**) Relation between spike trough-to-peak distance and entrainment to ictal spikes. For clarity, in **B** and **C** only neurons with firing rate >5 Hz are shown.

(Fig. 1E, and F; see Fig. 2C, and D for the KA model). Consistency of ictal patterns was evaluated by calculating ictal spike-triggered neuronal activity for each seizure (Fig. 1G) and computing the correlation coefficient between patterns in two consecutive seizures, similarly as described above. Correlation values for original data were significantly higher compared to neuron order shuffled data for all datasets ($r_{orig} = 0.53 \pm 0.074$, $r_{shufl} = 0.24 \pm 0.085$, $P = 0.0007$, *t*-test; Fig. 1H and Supplementary Fig. 6B). These results show that, similar to seizure-long patterns that appeared on slower time scales of tens of seconds, ictal spike-associated faster patterns were also strongly conserved across seizures.

In such ictal sequences, hippocampal neurons were usually active before neocortical neurons [average lag from the ictal spike peak: hippocampal (HP) neurons: 5.3 ms; parietal cortex (ParCtx) neurons: 10.5 ms; $P = 0.022$, *t*-test; note that for the latter analysis, hippocampal LFP from the tetrode with the highest amplitude ictal spikes was chosen]. In addition, the consistent sequential order was also observed if analyses were done separately for hippocampal neurons and neocortical neurons

($r_{origHP} = 0.47 \pm 0.07$, $r_{shuflHP} = 0.24 \pm 0.03$; $P = 0.006$; $r_{origParCtx} = 0.25 \pm 0.09$, $r_{shuflParCtx} = 0.1 \pm 0.05$, $P = 0.035$; *t*-test). Thus, consistent sequential patterns during ictal spikes reflected both timing differences between brain structures and sequential activity within a local area.

Ictal spikes preferentially entrain fast spiking cells

Next, we investigated the involvement of different cell types in ictal activity. Because a key class of GABAergic interneurons, the fast spiking cells, are known to have spike waveforms that are narrower than pyramidal cells (Barthó *et al.*, 2004), we measured spike half-width and trough-to-peak times for all recorded cells in order to distinguish interneurons (Fig. 3A). To provide additional support for the spike duration-based classification, we also quantified other cell properties indicative of cell class, including firing rate, shape of auto-correlogram and cross-correlogram (Fig. 3A, insets). We found that the majority of neurons that had a combination of high firing rate, cross-correlograms indicative of monosynaptic inhibition and auto-correlograms with a peak between 7 and 40 ms, also had narrow spikes with short trough-to-peak times <0.23 ms (Fig. 3A). This consistency between different measures indicated the validity of the cell type classification method.

Moreover, to determine the consistency of spike waveforms throughout the seizures for each cell type, we analysed the spike amplitude for all neurons. The data showed that during seizures, the average spike amplitude did not change significantly for the putative interneurons, and it decreased by ~2–5% for putative pyramidal cells (Supplementary Fig. 4). These findings are consistent with previous observations from human focal epilepsy, where similarly small spike amplitude reduction was observed (Truccolo *et al.*, 2011). *In vitro* and *in vivo* studies showed that decreases in spike amplitude could be caused by depolarization block (Bragin *et al.*, 1997; Bikson *et al.*, 2003; Ziburkus *et al.*, 2006); however, the decrease in spike amplitude that we observed was considerably smaller than what would be expected from depolarization block. Altogether, these data show that we could reliably record from both types of neurons throughout the seizure and that depolarization block was unlikely to play a key role in the activity of the recorded neurons.

Subsequently, we quantified the entrainment of each neuron to ictal spikes, by measuring the peak value of normalized cross-correlograms between spiking activity and hippocampal LFP (see 'Materials and methods' section for details). We found that putative interneurons (spike half-width <0.14 ms) had significantly higher entrainment values than putative pyramidal cells (spike half-width >0.14 ms) for both hippocampal and neocortical cells (Fig. 3B; $P < 0.001$ for both hippocampal and parietal cortex cells; Kolmogorov-Smirnov test; changing the half-width discrimination criteria by ± 0.02 ms gave similar results). Using trough-to-peak time values as discriminator between putative pyramidal neurons and interneurons gave similar results to the half-width measure [Fig. 3C; $P < 0.001$ for both hippocampal and parietal cortex cells; Kolmogorov-Smirnov test for putative interneurons (trough-to-peak time <0.23 ms) and putative pyramidal cells (>0.23 ms); changing trough-to-peak distance criteria by ± 0.02 ms gave similar results]. In addition, to avoid assigning specific threshold values for discriminating putative interneurons and pyramidal cells, we repeated the above analyses using a correlation coefficient measure. We found significant negative correlation between entrainment to ictal spikes and half-width of spikes for both hippocampal and cortical cells (hippocampal: $r = -0.63$, $P < 0.001$; cortical: $r = 0.6$, $P < 0.001$). Similar negative correlation was found for entrainment and trough-to-peak time as well (hippocampal: $r = -0.58$, $P < 0.001$; parietal cortex: $r = -0.64$, $P < 0.001$). The preferential entrainment of fast-spiking cells into ictal sequences was present both in the initial as in the late phase of seizures but was most evident at the later phases of seizure (Supplementary Fig. 8). These results showed that ictal spikes preferentially entrained fast spiking cells throughout the seizure.

Preferential strengthening of the strongest neuronal couplings during seizure

Next, we investigated if neuronal activity before seizures could predict neuronal entrainment to ictal spikes. The analysis showed that the strength of entrainment to ictal spikes was indeed dependent on the strength of neuronal coupling to LFP before seizure. Figure 4 illustrates that neuronal entrainment to hippocampal LFP before seizures (−5 min to 0 min) and during seizures was highly correlated for both hippocampal and parietal cells (hippocampal: $r = 0.48$, $P < 0.001$; parietal cortex: $r = 0.51$, $P < 0.001$), with putative interneurons having higher entrainment values (Supplementary Fig. 5A). The correlation between neuronal entrainment to LFP before and during the seizures was significant both during the initial and late phase of the seizure (Supplementary Fig. 9B). For putative pyramidal cells, we found no significant correlation between firing rate and LFP entrainment, suggesting that values of neuronal entrainment to LFP could not be simply explained by neuronal excitability (Supplementary Fig. 9C). In summary, these data indicate that neurons most modulated by hippocampal LFP before seizures were also most entrained to ictal spikes.

To investigate further the relationship between preictal and ictal neuronal activity patterns, we compared cross-correlograms for each pair of individual neurons between preictal (5 min to 0 min before seizure onset) and ictal periods. All cross-correlograms were normalized for firing rate and baseline subtracted, such that zero represented

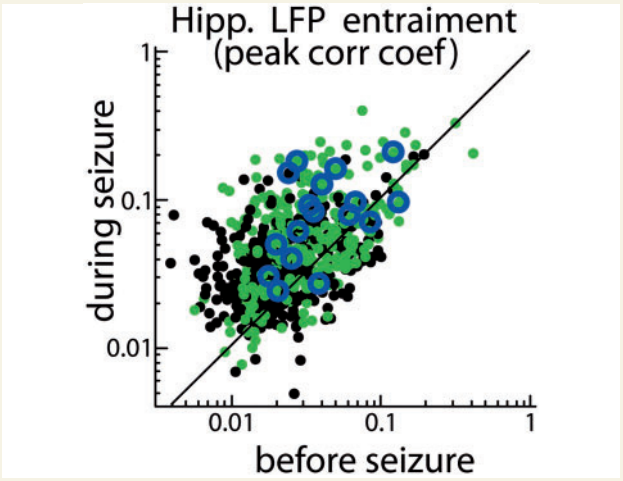

Figure 4 Relationship between the neuronal entrainment to hippocampal LFP before and during seizures. Each dot represents a single cell. Hippocampal and parietal cortex cells are marked in green and black, respectively. Blue circles denote cells that had in conjuncture three other typical features of interneurons (firing rate > 15 Hz, short latency inhibition to other cell, and most often inter-spike interval between 7 and 40 ms). Note that distributions of points along identity line shows that neurons more entrained to LFP before seizure are more likely to participate in ictal spikes.

cross-correlation expected by chance (Fig. 5A). The largest peaks in cross-correlograms were usually during seizure periods (Fig. 5A). Interestingly, the peak height of cross-correlogram during seizures correlated with peak height in the preictal period (Fig. 5B). This shows that the cross-correlogram peak during seizures depends on its magnitude before a seizure. Thus strongly correlated neurons during seizures are already (strongly) correlated during the preictal phase. The distribution of correlation coefficients was significantly different from what would be expected by chance from shuffled data of the correlation coefficients of the neuronal pairs [$r_{orig} = 0.22 \pm 0.04$, $r_{shufl} = 0.003 \pm 0.007$, $P < 0.0001$; *t*-test; Fig. 5C and D; note that the shuffled data here designate the correlation coefficients between neuronal pairs, which are different for preictal and ictal periods, e.g. preictal cross-correlation peaks (n1-n2, n1-n3, n1-n4, ...) and ictal cross-correlation peaks (n1-n6, n1-n9, n1-n2, ...), where n1-n2, etc denote the peak of cross-correlogram between neurons 1 and 2; note also that similar results were obtained when spike-time shuffled data were used as control]. Correlation between preictal and ictal cross-correlogram peaks was even higher when calculated between a single neuron and multi-unit activity [$r = 0.74 \pm 0.05$, $P < 0.0001$; *t*-test; mean slope = 2.6 ± 0.48, Fig. 5F and G; note that, for each cross-correlogram between a single neuron and multi-unit activity, we calculated multi-unit activity as the summed activity of all other simultaneously recorded cells, thus the multi-unit activity did not include the analysed neuron (Luczak *et al.*, 2009; Bermudez Contreras *et al.*, 2013)]. Examining the pre-ictal period 5 min to 2.5 min before a seizure (excluding 2.5 min of activity immediately before seizure) gave qualitatively similar results. Therefore, a measure of neuronal coupling to multi-unit activity or to LFP in the seizure-free period can provide a reliable estimate of which particular neurons will be most entrained to ictal spikes.

Next, we further analysed similarities in temporal structure between pre-ictal and ictal patterns. We again used pairwise cross-correlograms as in Fig. 5A, but each cross-correlogram was normalized between 0 and 1 to compare its overall shape. To reduce the effect of noise, only cross-correlograms that had more than 300 spikes within −50 +50 ms window were analysed, and cross-correlograms were smoothed with Gaussian kernel with 5 ms SD. Representative examples of normalized pairwise cross-correlograms for pre-ictal and ictal periods are shown in Fig. 6A and B, respectively. To compare the structure of cross-correlograms, we used again the methodology described in Supplementary Fig. 7. We found that the correlations between pre-ictal and ictal cross-correlogram patterns were higher as compared to order shuffled data for all analysed datasets ($r_{orig} = 0.29 \pm 0.063$, $r_{shufl} = 0.15 \pm 0.049$, $P = 0.0018$; paired *t*-test, Fig. 6C and D). Correlations between pre-ictal and ictal cross-correlogram patterns were consistent for both the initial and the late phase of seizure (Supplementary Fig. 10). We also applied an alternative method to quantify cross-correlogram similarities called 'latency' (Bermudez Contreras *et al.*, 2013), which gave qualitatively similar results (data not shown). Altogether, these results show that fine scale temporal relations between neurons before and during seizures were similar.

Discussion

Ictal sequences and fast spiking cells

The current study used tetrode recordings and rigorous analytical methods to examine the functional organization of large numbers of neurons in two brain areas in two rat models of chronic TLE. A major finding of the study is that neurons are often organized in temporal sequences during chronic seizures, and that such ictal sequences of firing involve a sizable population of fast spiking cells. While GABAergic interneurons are known to play crucial roles in epilepsy, their exact contribution to various seizure phenomena are still incompletely understood. For example, it is generally assumed that some form of functional imbalance must take place between excitation and inhibition in seizures, but precisely how such imbalance may be generated in mechanistic terms is unclear. Indeed, while there is an abundance of evidence indicating various forms of compromised inhibitory systems in hyperexcitable circuits, including GABAergic cell loss (Obenaus *et al.*, 1993; Cossart *et al.*, 2001; Santhakumar *et al.*, 2001; Kobayashi and Buckmaster, 2003), the appearance of depolarizing GABA responses during heightened levels of

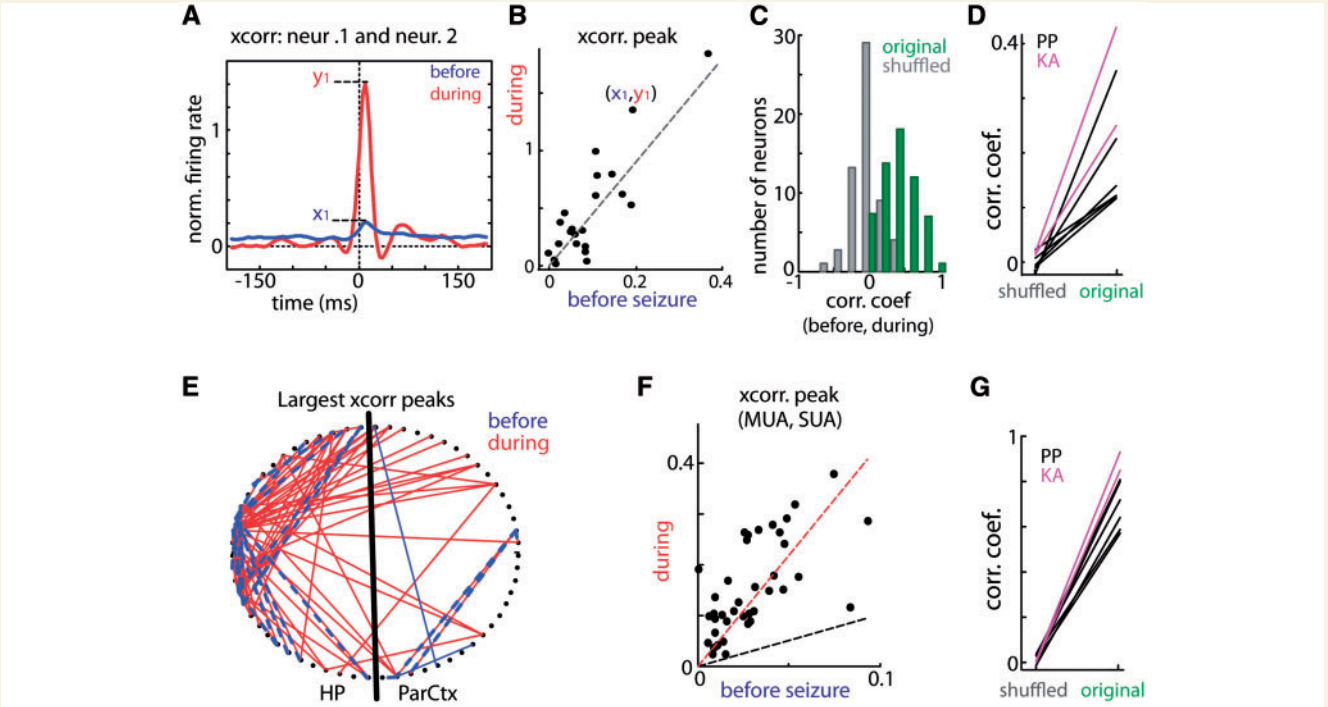

Figure 5 Neuronal interactions before and during seizure are correlated. (**A**) Example of pair-wise cross-correlograms between two neurons before and during seizure. (**B**) Size of cross-correlogram peak before and during seizure for an analysed sample neuron. Each dot corresponds to a pair of neurons: the analysed neuron and one other neuron. Point labelled with (x1,y1) corresponds to peaks shown in **A**. Dashed line represent regression lines (without offset term). (**C**) Distribution of correlation coefficient values between cross-correlogram peaks before and during seizure for a representative dataset (original data: green bars; neuron-shuffled data: grey bars). (**D**) Average correlation coefficient between cross-correlogram peaks before and during seizure for all datasets. Plot convention the same as in Fig. 1D. (**E**) Spatial distribution of strong neuronal interactions before (blue), and during seizure (red) in a representative dataset. Each black dot represents a single neuron, with hippocampal (HP) neurons plotted on left side and parietal neurons on right side (ParCtx). Lines denote which neuronal pairs had large peak (>0.5) in cross-correlogram. Note that most neurons with strong interactions before seizure were also highly correlated during seizure (marked by dashed lines). (**F**) Size of peak in cross-correlograms between single neuron (SUA) and multiunit activity (MUA) for representative dataset. (**G**) Correlation coefficient between SUA–MUA cross-correlogram peaks before and during seizure for all datasets. Plot convention the same as in Fig. 1D. In **D** and **G**, higher values of correlation for all original datasets as compared to shuffled data, shows that 'coupling' between neurons during seizures, consistently emerged between neurons, which already had stronger correlations before the seizure.

activity (Kaila *et al.*, 2014; Staley, 2015), a possible depolarization block of interneurons during ictal events (Ahmed *et al.*, 2014; Karlócai *et al.*, 2014), and that closed-loop optogenetic activation of fast spiking interneurons can effectively curtail both electrographic and behavioural seizures in experimental TLE (Krook-Magnuson *et al.*, 2013); however, increased inhibitory activity during seizure initiation has also been reported, which indicates a more complex role for inhibition (Sessolo *et al.*, 2015; Shiri *et al.*, 2015; Lévesque *et al.*, 2016*b*; Khoshkhoo *et al.*, 2017).

Our data, demonstrating the presence of spontaneous ictal sequences with significant participation by fast spiking cells, are in agreement with a recent study showing that interictal spikes are dominated by GABAergic neuronal activity in chronic experimental TLE (Muldoon *et al.*, 2015). Fast spikes in cortical networks are characteristic of parvalbumin-expressing interneurons that powerfully regulate perisomatic and proximal dendritic inhibition in the normal brain (Armstrong and Soltesz, 2012; Hu *et al.*, 2014). Interestingly, a key feature of such fast spiking interneurons is that they receive large numbers of excitatory inputs both from local principal cells as well as from afferent sources (Szabadics and Soltesz, 2009; Isaacson and Scanziani, 2011). Moreover, fast spiking interneurons have lower spiking threshold, they are strongly entrained to hippocampal theta (Fox and Ranck, 1975) and to other hippocampal LFP rhythms (Varga *et al.*, 2012), and are readily activated by stimulation of afferents (Mizumori *et al.*, 1989*b*), consistent with the notion that due to their broad selectivity they can be preferentially activated by a variety of inputs. Therefore, it is conceivable that the prominent presence of fast spiking unit activity in ictal sequences observed in our recordings reflect the arrival of ictal wavefronts from areas adjacent to the electrodes (Smith *et al.*, 2016). In addition, synapses between fast spiking interneurons (Freund and Buzsáki, 1996; Bartos *et al.*, 2007), and interactions with recurrently connected excitatory cells (Tsodyks *et al.*, 1997) may also play a role in shaping the temporal sequence of unit firing in ictal events. Moreover,

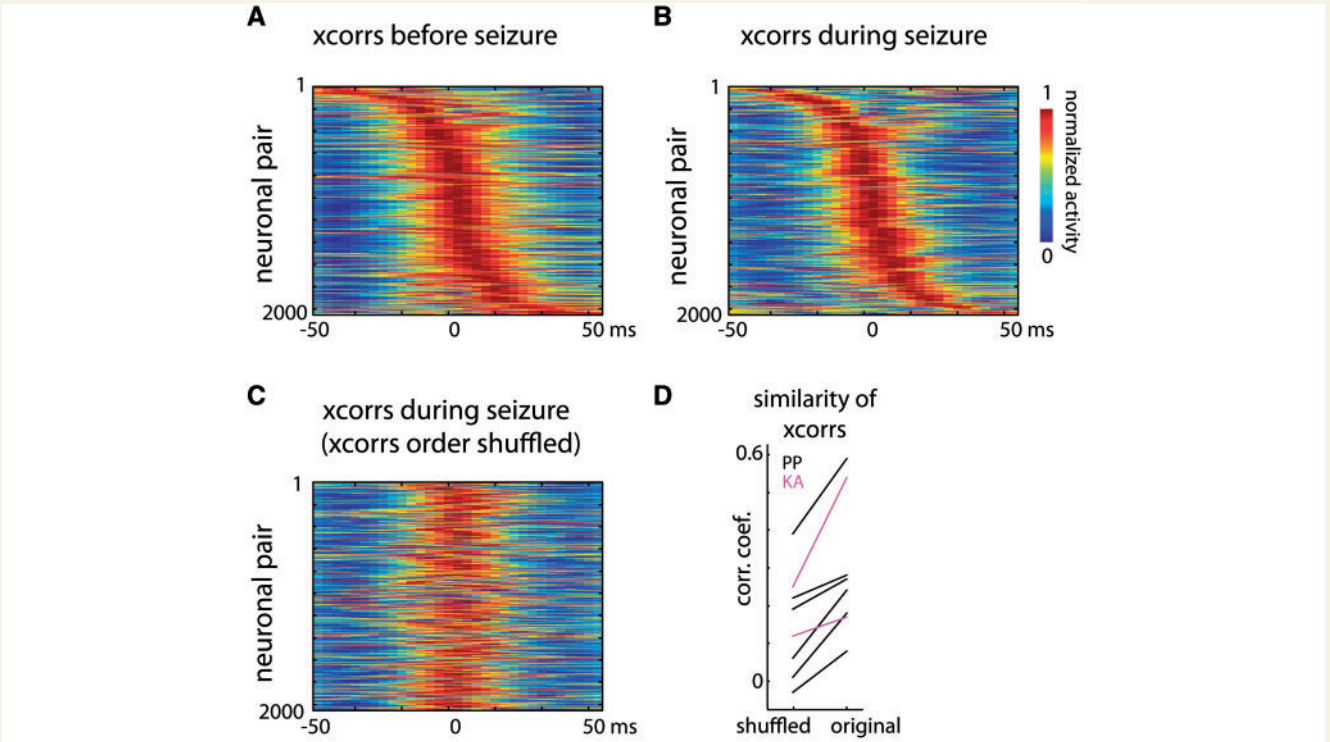

Figure 6 Temporal activity patterns before and during seizure are similar. (**A**) Two thousand cross-correlograms between pairs of neurons calculated during −5:0 min periods before seizures in a single experiment. (**B**) Cross-correlograms between the same pairs of neurons as in **A** but during seizures. Cross-correlograms in **A** and **B** are sorted in the same order. Each cross-correlogram was smoothed with 5 ms Gaussian kernel and normalized between 0 and 1. **A** and **B** represent average cross-correlograms across all preseizure and seizure periods respectively, in a single 24 h recording. (**C**) Same as **B** but with shuffled order of cross-correlograms. (**D**) Correlation coefficients between cross-correlograms calculated before and during seizures. For all datasets, the similarity between the original patterns was higher compared to the cross-correlogram order shuffled data.

several studies have indicated the involvement of some form of synchronized GABAergic activity in seizure generation (Avoli, 1996; Gnatkovsky *et al.*, 2008; Fujiwara-Tsukamoto *et al.*, 2010; Ellender *et al.*, 2014; Uva *et al.*, 2015; for review see Curtis and Avoli, 2016), and increased synchronization of interneurons with LFP has been reported to occur even minutes before seizure onset (Grasse *et al.*, 2013). It should be noted that future studies will be needed to determine to what extent the action potential discharges by the fast spiking, presumed GABAergic, interneurons during ictal and interictal events translate to effective inhibition on principal cell excitability and shape seizure characteristics such as duration and termination.

Relationship between interictal and ictal sequences

Our results indicate that neurons that are highly coupled to population activity before seizures are the ones that are preferentially involved in ictal events. Thus, measures of neuronal coupling to multi-unit activity or to LFP in interictal periods may help to identify and predict neurons most involved in ictal activity. Our data indicating that correlation patterns between neurons are similar before and during a seizure provide insights into the nature of pre-ictal and ictal activity patterns and show predominant role of interneurons in seizure dynamics. Interestingly, subsets of neurons strongly coupled to population activity were also reported in sensory cortex of non-epileptic animals (Okun *et al.*, 2015), with the participating neurons being more strongly activated by a variety of sensory stimuli, polysynaptic optogenetic stimulation, and top-down modulation. Most of those neurons were putative interneurons, which is consistent with properties of GABAergic cells described above and with our results presented here. This suggests that in epilepsy, such strongly correlated neurons could form a strongly connected network, which may facilitate propagation of epileptic activity.

Although similar correlations between neurons during non-ictal and ictal patterns in some sense may not be entirely unexpected, it should be noted that each neuron receives input from hundreds and even thousands of presynaptic neurons that, at least in principle, could provide cortical circuits with the potential to generate a very large number of different patterns, where small changes in inputs or behavioural state may lead to the emergence of distinct activity patterns. Thus, it was rather surprising that studies in the normal brain have revealed similarities

between activity patterns across different conditions (e.g. memory replay: Wilson and McNaughton, 1994; spontaneous and stimulus evoked patterns: Kenet *et al.*, 2003; Luczak *et al.*, 2015). Future experimental and theoretical investigations will be needed to understand how normal neuronal sequences and epilepsy-related patterns during non-ictal and ictal periods interrelate in mechanistic terms.

Limitations

While the present study revealed novel insights into the existence of ictal sequences with a strong participation by fast spiking units in spontaneous chronic seizures, the experimental paradigm that was employed, naturally, also came with significant caveats that should be taken into account. Among the major limitations of the approach is the fact that, although high density neuronal recordings with hyperdrives allows recordings with high spatial and temporal resolution, the overall sampling coverage is low. A closely related question is whether we recorded from the seizure focus. Defining the seizure focus is not always straightforward; indeed, to our knowledge, it has never been demonstrated that a small group of neurons (the focus) reliably initiates focal seizures *in vivo*. The latter hypothesis concerning the focus is especially difficult to test with hyperdrive recordings, because the onset of seizures could in principle always be far from the recording electrode. Indeed, seizures may be associated with specific interactions between nodes of widespread brain networks (Nadler and Spencer, 2014; Kimchi and Cash, 2015) as seen in combined EEG and functional MRI recordings (Federico *et al.*, 2005) and depth and cortical surface EEG recordings (Perucca *et al.*, 2013; Khambhati *et al.*, 2015), suggesting that the concept of focus as the origin of a seizure may be more properly substituted by the concept of networks. In addition, as seizures propagate through cerebral networks, microcircuits in distal nodes can be engaged, and subsets of neurons in seemingly distal nodes, away from the *de facto* seizure focus, can have surprisingly powerful control over the outcome of the seizure (Krook-Magnuson *et al.*, 2014; Paz and Huguenard, 2015). Our recordings most likely did not take place from within the seizure focus, since we mainly sampled from parietal cortex and dorsal hippocampus, and various studies suggested that while seizures in the intraperitoneal pilocarpine and kainate chemoconvulsant models of TLE typically do not have a single focus for every seizure, the ictal events predominantly originate from the ventral hippocampus, subiculum, dentate gyrus and entorhinal cortex (Bragin *et al.*, 2005; Boido *et al.*, 2012; Goldberg and Coulter, 2013; Toyoda *et al.*, 2015). Another argument supporting the notion that we were recording from outside the seizure focus is that we were able to reliably sort spikes throughout the seizures, while such reliable sorting is reportedly extremely challenging in the case of recordings from seizure foci due to hypersynchronous neuronal activation and paroxysmal depolarization shifts (Merricks *et al.*, 2015). Indeed we did not observe hypersynchronous firing of all neurons, despite clear ictal discharges on the LFP signal. This is in line with other studies that recorded activity of individual neurons in relation to epileptic seizures (Bower and Buckmaster, 2008; Truccolo *et al.*, 2011; Bower *et al.*, 2012; Ewell *et al.*, 2015). Therefore, our results most likely reflect neuronal activity patterns as invading ictal wavefronts engage the local dorsal hippocampal and neocortical microcircuits.

A second major technical limitation concerns the relatively low number of animals from which our dataset originates. Hyperdrive recordings are notoriously difficult and time consuming; therefore, studies using this technique usually collect data from only two to four animals [e.g. two rats (Euston *et al.*, 2007); three rats (Wang *et al.*, 2015); two rats in each of two groups (Steiner and Redish, 2014); three rats (Winter *et al.*, 2015)]. We obtained high quality recordings from three rats using the perforant path stimulation (PP) model of chronic TLE, and from one rat in the kainic acid (KA) model. Although it is often difficult to compare across experimental models, our data from the PP and KA models indicate surprisingly consistent and reproducible results, which, together with the large number of seizures recorded in both models, and the quantitative analytical approaches supported by unbiased statistical methods, increase the confidence in the conclusions.

Third, it should be noted that, in experiments with extracellular tetrode recordings, correct assignment of spikes to single neurons can be sometimes challenging, especially during seizures. Although we have considerable experience with extracellular recordings (McNaughton *et al.*, 1983; Luczak and Narayanan, 2005; Schjetnan and Luczak, 2011; Schwindel *et al.*, 2014), and we worked with well-isolated units with consistent waveforms throughout ictal and pre-ictal periods (Supplementary Figs 3 and 4), we also likely had a significant number of misclassified spikes. Importantly, however, our results are highly unlikely to be due to problems with spike sorting. Errors in spike sorting would likely reduce significance of our findings, rather than causing false-positive results. For example, it is unlikely that narrow spike cell clusters would contain significant number of spikes from principal cells, because adding principal cell spikes would result in broadening (not thinning) of the average spike waveform. Moreover, the consistency of cross-correlograms before and during seizures strongly suggests that we isolated the same units in both periods. Indeed, errors in spike sorting would be expected to result in a decreased probability of finding consistent temporal relations between neurons in pre-ictal and ictal periods. A similar reasoning would also apply to the similarity of patterns across seizures (Figs 1 and 2), where errors in assignments of spikes to clusters would reduce, rather than enhance, the similarity of neuronal sequences across seizures. Therefore, although errors in spike sorting are unavoidable, such errors were unlikely to give rise to the correlations that were observed.

Outlook

In this study, we show similarities between ictal and pre-ictal patterns of neuronal activity. Interestingly, the similarity of ictal and pre-ictal patterns indicate that it may be possible to study ictal-like sequences even during periods between seizures. Spontaneous seizures often occur quite rarely in both epileptic patients (Leidy *et al.*, 1999) and animal models of TLE (Gorter *et al.*, 2001; Raedt *et al.*, 2009; Ewell *et al.*, 2015). This relative infrequency of spontaneous seizures significantly limits the amount of data that can be obtained to study epileptic networks in individual subjects reliably. By showing that seizure-related patterns are also present in activity between seizures, our results indicate a potential opportunity to gather significantly more data to examine epileptic circuits in order to assist future individualized treatment modalities. For example, one may speculate that by monitoring neurons most entrained to LFP during spontaneous sequential patterns outside of ictal events, it may be one day possible to reliably predict propagation patterns of ictal activity even if actual seizures are not observed in the epilepsy monitoring unit. Although more research is needed to make such a vision a reality, it is interesting to note that induced focal seizures in the visual cortex have been observed to propagate along functional connectivity that also underlies normal visual processing (Rossi *et al.*, 2016). Thus, investigation of network activity during non-ictal periods may one day provide clues about epileptic networks in cases when ictal data are scarce.

Acknowledgements

We thank Sisay Yimenu and Cindy Hoang for technical assistance, and Majid Mohajerani for helpful comments.

Funding

This research was supported by the Alberta Innovates Health Solutions Polaris Award and National Science Foundation grant (1631465) to B.L.M., Natural Sciences and Engineering Research Council of Canada Discovery Grant and Accelerator Supplement to A.L., BLM, BOF to R.R. and K.V., FWO-aspirant grant from Research Foundation Flanders to M.S., and grants from FWO, BOF and by the Clinical Epilepsy Grant from Ghent University Hospital to P.B. and by the National Institutes of Health (NS35915) to I.S.

Supplementary material

Supplementary material is available at *Brain* online.

References

Ahmed OJ, Kramer MA, Truccolo W, Naftulin JS, Potter NS, Eskandar EN, et al. Inhibitory single neuron control of seizures and epileptic traveling waves in humans. BMC Neurosci 2014; 15: F3.

Armstrong C, Soltesz I. Basket cell dichotomy in microcircuit function. J Physiol 2012; 590: 683–94.

Avoli M. GABA-mediated synchronous potentials and seizure generation. Epilepsia 1996; 37: 1035–42.

Barthó P, Hirase H, Monconduit L, Zugaro M, Harris KD, Buzsáki G. Characterization of neocortical principal cells and interneurons by network interactions and extracellular features. J Neurophysiol 2004; 92: 600–8.

Bartos M, Vida I, Jonas P. Synaptic mechanisms of synchronized gamma oscillations in inhibitory interneuron networks. Nat Rev Neurosci 2007; 8: 45–56.

Bermudez Contreras EJ, Schjetnan AGP, Muhammad A, Bartho P, McNaughton BL, Kolb B, et al. Formation and reverberation of sequential neural activity patterns evoked by sensory stimulation are enhanced during cortical desynchronization. Neuron 2013; 79: 555–66.

Bikson M, Hahn PJ, Fox JE, Jefferys JG. Depolarization block of neurons during maintenance of electrographic seizures. J Neurophysiol 2003; 90: 2402–8.

Boido D, Jesuthasan N, de Curtis M, Uva L. Network dynamics during the progression of seizure-like events in the hippocampal–parahippocampal regions. Cereb Cortex 2012; 24: 163–73.

Bower MR, Buckmaster PS. Changes in granule cell firing rates precede locally recorded spontaneous seizures by minutes in an animal model of temporal lobe epilepsy. J Neurophysiol 2008; 99: 2431–42.

Bower MR, Stead M, Meyer FB, Marsh WR, Worrell GA. Spatiotemporal neuronal correlates of seizure generation in focal epilepsy. Epilepsia 2012; 53: 807–16.

Bragin A, Azizyan A, Almajano J, Wilson CL, Engel J. Analysis of chronic seizure onsets after intrahippocampal kainic acid injection in freely moving rats. Epilepsia 2005; 46: 1592–8.

Bragin A, Engel J, Wilson CL, Vizentin E, Mathern GW. Electrophysiologic analysis of a chronic seizure model after unilateral hippocampal KA injection. Epilepsia 1999; 40: 1210–21.

Bragin A, Penttonen M, Buzsáki G. Termination of epileptic afterdischarge in the hippocampus. J Neurosci 1997; 17: 2567–79.

Bumanglag AV, Sloviter RS. Minimal latency to hippocampal epileptogenesis and clinical epilepsy after perforant pathway stimulation-induced status epilepticus in awake rats. J Comp Neurol 2008; 510: 561–80.

Buzsáki G, Chen LS, Gage FH. Chapter spatial organization of physiological activity in the hippocampal region: relevance to memory formation. Prog Brain Res 1990; 83: 257–68.

Cardin JA, Carlén M, Meletis K, Knoblich U, Zhang F, Deisseroth K, et al. Driving fast-spiking cells induces gamma rhythm and controls sensory responses. Nature 2009; 459: 663–7.

Chen K, Aradi I, Thon N, Eghbal-Ahmadi M, Baram TZ, Soltesz I. Persistently modified h-channels after complex febrile seizures convert the seizure-induced enhancement of inhibition to hyperexcitability. Nat Med 2001; 7: 331–7.

Cohen I, Navarro V, Clemenceau S, Baulac M, Miles R. On the origin of interictal activity in human temporal lobe epilepsy *in vitro*. Science 2002; 298: 1418–21.

Cossart R, Dinocourt C, Hirsch J, Merchan-Perez A, De Felipe J, Ben-Ari Y, et al. Dendritic but not somatic GABAergic inhibition is decreased in experimental epilepsy. Nat Neurosci 2001; 4: 52–62.

Curtis M, Avoli M. GABAergic networks jump-start focal seizures. Epilepsia 2016; 57: 679–87.

Cymerblit-Sabba A, Schiller Y. Development of hypersynchrony in the cortical network during chemoconvulsant-induced epileptic seizures *in vivo*. J Neurophysiol 2012; 107: 1718–30.

Ellender TJ, Raimondo JV, Irkle A, Lamsa KP, Akerman CJ. Excitatory effects of parvalbumin-expressing interneurons maintain hippocampal epileptiform activity via synchronous afterdischarges. J Neurosci 2014; 34: 15208–22.

Euston DR, Tatsuno M, McNaughton BL. Fast-forward playback of recent memory sequences in prefrontal cortex during sleep. Science 2007; 318: 1147–50.

Ewell LA, Liang L, Armstrong C, Soltész I, Leutgeb S, Leutgeb JK. Brain state is a major factor in preseizure hippocampal network activity and influences success of seizure intervention. J Neurosci 2015; 35: 15635–48.

Federico P, Abbott DF, Briellmann RS, Harvey AS, Jackson GD. Functional MRI of the pre-ictal state. Brain 2005; 128: 1811–17.

Fox SE, Ranck J. Localization and anatomical identification of theta and complex spike cells in dorsal hippocampal formation of rats. Exp Neurol 1975; 49: 299–313.

Freund TF, Buzsáki G. Interneurons of the hippocampus. Hippocampus 1996; 6: 347–470.

Fujiwara-Tsukamoto Y, Isomura Y, Imanishi M, Ninomiya T, Tsukada M, Yanagawa Y, et al. Prototypic seizure activity driven by mature hippocampal fast-spiking interneurons. J Neurosci 2010; 30: 13679–89.

Gnatkovsky V, Librizzi L, Trombin F, de Curtis M. Fast activity at seizure onset is mediated by inhibitory circuits in the entorhinal cortex *in vitro*. Ann Neurol 2008; 64: 674–86.

Goldberg EM, Coulter DA. Mechanisms of epileptogenesis: a convergence on neural circuit dysfunction. Nat Rev Neurosci 2013; 14: 337–49.

Gorter J, Van Vliet E, Aronica E, Da Silva F. Progression of spontaneous seizures after status epilepticus is associated with mossy fibre sprouting and extensive bilateral loss of hilar parvalbumin and somatostatin-immunoreactive neurons. Eur J Neurosci 2001; 13: 657–69.

Gothard KM, Skaggs WE, Moore KM, McNaughton BL. Binding of hippocampal CA1 neural activity to multiple reference frames in a landmark-based navigation task. J Neurosci 1996; 16: 823–35.

Grasse DW, Karunakaran S, Moxon KA. Neuronal synchrony and the transition to spontaneous seizures. Exp Neurol 2013; 248: 72–84.

Gray CM, Maldonado PE, Wilson M, McNaughton B. Tetrodes markedly improve the reliability and yield of multiple single-unit isolation from multi-unit recordings in cat striate cortex. J Neurosci Methods 1995; 63: 43–54.

Harris KD, Henze DA, Csicsvari J, Hirase H, Buzsáki G. Accuracy of tetrode spike separation as determined by simultaneous intracellular and extracellular measurements. J Neurophysiol 2000; 84: 401–14.

Hu H, Gan J, Jonas P. Fast-spiking, parvalbumin+ GABAergic interneurons: from cellular design to microcircuit function. Science 2014; 345: 1255263.

Isaacson JS, Scanziani M. How inhibition shapes cortical activity. Neuron 2011; 72: 231–43.

Kaila K, Ruusuvuori E, Seja P, Voipio J, Puskarjov M. GABA actions and ionic plasticity in epilepsy. Curr Opinion Neurobiol 2014; 26: 34–41.

Kandratavicius L, Balista PA, Lopes-Aguiar C, Ruggiero RN, Umeoka EH, Garcia-Cairasco N, et al. Animal models of epilepsy: use and limitations. Neuropsychiatr Dis Treat 2014; 10: 1693.

Karlócai MR, Kohus Z, Káli S, Ulbert I, Szabó G, Máté Z, et al. Physiological sharp wave-ripples and interictal events *in vitro*: what's the difference? Brain 2014: awt348.

Kenet T, Bibitchkov D, Tsodyks M, Grinvald A, Arieli A. Spontaneously emerging cortical representations of visual attributes. Nature 2003; 425: 954–6.

Khambhati AN, Davis KA, Oommen BS, Chen SH, Lucas TH, Litt B, et al. Dynamic network drivers of seizure generation, propagation and termination in human neocortical epilepsy. PLoS Comput Biol 2015; 11: e1004608.

Khoshkhoo S, Vogt D, Sohal VS. Dynamic, cell-type-specific roles for GABAergic interneurons in a mouse model of optogenetically inducible seizures. Neuron 2017; 93: 291–8.

Kimchi EY, Cash SS. Seizures at the scale of individual neurons. Brain 2015; 138: 2807–8.

Kobayashi M, Buckmaster PS. Reduced inhibition of dentate granule cells in a model of temporal lobe epilepsy. J Neurosci 2003; 23: 2440–52.

Krook-Magnuson E, Armstrong C, Oijala M, Soltesz I. On-demand optogenetic control of spontaneous seizures in temporal lobe epilepsy. Nat Commun 2013; 4: 1376.

Krook-Magnuson E, Szabo GG, Armstrong C, Oijala M, Soltesz I. Cerebellar directed optogenetic intervention inhibits spontaneous hippocampal seizures in a mouse model of temporal lobe epilepsy. eNeuro 2014; 1: pii: e.2014.

Leidy N, Elixhauser A, Vickrey B, Means E, Willian M. Seizure frequency and the health-related quality of life of adults with epilepsy. Neurology 1999; 53: 162–6.

Lévesque M, Avoli M, Bernard C. Animal models of temporal lobe epilepsy following systemic chemoconvulsant administration. J Neurosci Methods 2016a; 260: 45–52.

Lévesque M, Herrington R, Hamidi S, Avoli M. Interneurons spark seizure-like activity in the entorhinal cortex. Neurobiol Dis 2016b; 87: 91–101.

Luczak A, Barthó P. Consistent sequential activity across diverse forms of UP states under ketamine anesthesia. Eur J Neurosci 2012; 36: 2830–8.

Luczak A, Barthó P, Harris KD. Spontaneous events outline the realm of possible sensory responses in neocortical populations. Neuron 2009; 62: 413–25.

Luczak A, McNaughton BL, Harris KD. Packet-based communication in the cortex. Nature Rev Neurosci 2015; 16: 745–55.

Luczak A, Narayanan NS. Spectral representation—analyzing single-unit activity in extracellularly recorded neuronal data without spike sorting. J Neurosci Methods 2005; 144: 53–61.

Marchionni I, Maccaferri G. Quantitative dynamics and spatial profile of perisomatic GABAergic input during epileptiform synchronization in the CA1 hippocampus. J Physiol 2009; 587: 5691–708.

Markus EJ, Barnes CA, McNaughton BL, Gladden VL, Skaggs WE. Spatial information content and reliability of hippocampal CA1 neurons: effects of visual input. Hippocampus 1994; 4: 410–21.

McNaughton BL. Implantable multi-electrode microdrive array. U.S. Patent No. 5,928,143. Washington, DC: U.S. Patent and Trademark Office. 1999.

McNaughton BL, Douglas R, Goddard GV. Synaptic enhancement in fascia dentata: cooperativity among coactive afferents. Brain Res 1978; 157: 277–93.

McNaughton BL, O'Keefe J, Barnes CA. The stereotrode: a new technique for simultaneous isolation of several single units in the central nervous system from multiple unit records. J Neurosci Methods 1983; 8: 391–7.

Merricks EM, Smith EH, McKhann GM, Goodman RR, Bateman LM, Emerson RG, et al. Single unit action potentials in humans and the effect of seizure activity. Brain 2015; 138 (Pt 10): 2891–906.

Mizumori S, Barnes CA, McNaughton B. Reversible inactivation of the medial septum: selective effects on the spontaneous unit activity of different hippocampal cell types. Brain Res 1989a; 500: 99–106.

Mizumori S, Mcnaughton BL, Barnes CA. A comparison of supramammillary and medial septal influences on hippocampal field potentials and single-unit activity. J Neurophysiol 1989b; 61: 15–31.

Muldoon SF, Soltesz I, Cossart R. Spatially clustered neuronal assemblies comprise the microstructure of synchrony in chronically epileptic networks. Proc Natl Acad Sci USA 2013; 110: 3567–72.

Muldoon SF, Villette V, Tressard T, Malvache A, Reichinnek S, Bartolomei F, et al. GABAergic inhibition shapes interictal dynamics in awake epileptic mice. Brain 2015; 138: 2875–90.

Nadler JV, Spencer DD. What is a seizure focus? Issues in clinical epileptology: a view from the bench. The Netherlands: Springer; 2014. p. 55–62.
Obenaus A, Esclapez M, Houser C. Loss of glutamate decarboxylase mRNA-containing neurons in the rat dentate gyrus following pilocarpine-induced seizures. J Neurosci 1993; 13: 4470–85.
Okun M, Steinmetz NA, Cossell L, Iacaruso MF, Ko H, Barthó P, et al. Diverse coupling of neurons to populations in sensory cortex. Nature 2015; 521: 511–15.
Paz JT, Huguenard JR. Microcircuits and their interactions in epilepsy: is the focus out of focus? Nat Neurosci 2015; 18: 351–9.
Perucca P, Dubeau F, Gotman J. Widespread EEG changes precede focal seizures. PLoS One 2013; 8: e80972.
Prince DA. Inhibition in "epileptic" neurons. Exp Neurol 1968; 21: 307–21.
Prince DA, Wilder BJ. Control mechanisms in cortical epileptogenic foci*: surround inhibition. Arch Neurol 1967; 16: 194–202.
Racine RJ. Modification of seizure activity by electrical stimulation: II. Motor seizure. Electroencephalogr Clin Neurophysiol 1972; 32: 281–94.
Raedt R, Van Dycke A, Van Melkebeke D, De Smedt T, Claeys P, Wyckhuys T, et al. Seizures in the intrahippocampal kainic acid epilepsy model: characterization using long-term video-EEG monitoring in the rat. Acta Neurol Scand 2009; 119: 293–303.
Redish AD. MClust Spike Sorting Toolbox. 2002. Available from: http://wwwcbcumnedu/~redish/mclust.
Rossi LF, Wykes RC, Kullman D, Carandini M. Cortical seizure propagation respects functional connectivity underlying sensory processing. bioRxiv 2016: 080598.
Sabolek HR, Swiercz WB, Lillis KP, Cash SS, Huberfeld G, Zhao G, et al. A candidate mechanism underlying the variance of interictal spike propagation. J Neurosci 2012; 32: 3009–21.
Santhakumar V, Ratzliff AD, Jeng J, Toth Z, Soltesz I. Long-term hyperexcitability in the hippocampus after experimental head trauma. Ann Neurol 2001; 50: 708–17.
Schevon CA, Weiss SA, McKhann G Jr, Goodman RR, Yuste R, Emerson RG, et al. Evidence of an inhibitory restraint of seizure activity in humans. Nat Commun 2012; 3: 1060.
Schjetnan AG, Luczak A. Recording large-scale neuronal ensembles with silicon probes in the anesthetized rat. J Vis Exp 2011; 56: 3282.
Schwindel CD, Ali K, McNaughton BL, Tatsuno M. Long-term recordings improve the detection of weak excitatory–excitatory connections in rat prefrontal cortex. J Neurosci 2014; 34: 5454–67.
Sessolo M, Marcon I, Bovetti S, Losi G, Cammarota M, Ratto GM, et al. Parvalbumin-positive inhibitory interneurons oppose propagation but favor generation of focal epileptiform activity. J Neurosci 2015; 35: 9544–57.
Shiri Z, Manseau F, Lévesque M, Williams S, Avoli M. Interneuron activity leads to initiation of low-voltage fast-onset seizures. Ann Neurol 2015; 77: 541–6.
Smith EH, Liou JY, Davis TS, Merricks EM, Kellis SS, Weiss SA, et al. The ictal wavefront is the spatiotemporal source of discharges during spontaneous human seizures. Nat Commun 2016; 7: 11098.
Staley K. Molecular mechanisms of epilepsy. Nat Neurosci 2015; 18: 367–72.
Stark E, Roux L, Eichler R, Senzai Y, Royer S, Buzsáki G. Pyramidal cell-interneuron interactions underlie hippocampal ripple oscillations. Neuron 2014; 83: 467–80.
Steiner AP, Redish AD. Behavioral and neurophysiological correlates of regret in rat decision-making on a neuroeconomic task. Nat Neurosci 2014; 17: 995–1002.
Szabadics J, Soltesz I. Functional specificity of mossy fiber innervation of GABAergic cells in the hippocampus. J Neurosci 2009; 29: 4239–51.
Thurman D, Beghi E, Begley C, Berg A, Buchhalter J, Ding D. Standards for epidemiologic studies and surveillance of epilepsy. Epilepsia 2011; 52 (Suppl 7): 2–26.
Toyoda I, Fujita S, Thamattoor AK, Buckmaster PS. Unit activity of hippocampal interneurons before spontaneous seizures in an animal model of temporal lobe epilepsy. J Neurosci 2015; 35: 6600–18.
Trevelyan AJ, Schevon CA. How inhibition influences seizure propagation. Neuropharmacology 2013; 69: 45–54.
Trevelyan AJ, Sussillo D, Watson BO, Yuste R. Modular propagation of epileptiform activity: evidence for an inhibitory veto in neocortex. J Neurosci 2006; 26: 12447–55.
Truccolo W, Ahmed OJ, Harrison MT, Eskandar EN, Cosgrove GR, Madsen JR, et al. Neuronal ensemble synchrony during human focal seizures. J Neurosci 2014; 34: 9927–44.
Truccolo W, Donoghue JA, Hochberg LR, Eskandar EN, Madsen JR, Anderson WS, et al. Single-neuron dynamics in human focal epilepsy. Nat Neurosci 2011; 14: 635–41.
Tsodyks MV, Skaggs WE, Sejnowski TJ, McNaughton BL. Paradoxical effects of external modulation of inhibitory interneurons. J Neurosci 1997; 17: 4382–8.
Uva L, Breschi GL, Gnatkovsky V, Taverna S, de Curtis M. Synchronous inhibitory potentials precede seizure-like events in acute models of focal limbic seizures. J Neurosci 2015; 35: 3048–55.
Varga C, Golshani P, Soltesz I. Frequency-invariant temporal ordering of interneuronal discharges during hippocampal oscillations in awake mice. Proc Natl Acad Sci USA 2012; 109: E2726–34.
Velazquez JLP, Carlen PL. Synchronization of GABAergic interneuronal networks during seizure-like activity in the rat horizontal hippocampal slice. Eur J Neurosci 1999; 11: 4110–18.
Vermoesen K, Smolders I, Massie A, Michotte Y, Clinckers R. The control of kainic acid-induced status epilepticus. Epilepsy Res 2010; 90: 164–6.
Wang Y, Romani S, Lustig B, Leonardo A, Pastalkova E. Theta sequences are essential for internally generated hippocampal firing fields. Nat Neurosci 2015; 18: 282–8.
Wiebe S. Epidemiology of temporal lobe epilepsy. Can J Neurol Sci 2000; 27: S6–S10.
Wilson MA, McNaughton BL. Reactivation of hippocampal ensemble memories during sleep. Science 1994; 265: 676–9.
Winter SS, Clark BJ, Taube JS. Disruption of the head direction cell network impairs the parahippocampal grid cell signal. Science 2015; 347: 870–4.
Ziburkus J, Cressman JR, Barreto E, Schiff SJ. Interneuron and pyramidal cell interplay during *in vitro* seizure-like events. J Neurophysiol 2006; 95: 3948–54.